JOURNAL OF SOLID STATE CHEMISTRY 72, 100–112 (1988)

A Time of Flight Neutron Powder Rietveld Refinement Study at Elevated Temperature on a Monoclinic Near-Stoichiometric NASICON*

P. R. RUDOLF AND A. CLEARFIELD†

Department of Chemistry, Texas A&M University, College Station, Texas 77843

AND J. D. JORGENSEN

Materials Science and Technology Division, Argonne National Laboratory, Argonne, Illinois 60434

Received March 2, 1987

Time of flight neutron powder data were collected at elevated temperatures on a sample of NASICON of composition $Na_{3.17}Zr_{1.93}Si_{1.9}P_{1.1}O_{12}$. This sample, prepared by reheating a commerically available NASICON to minimize the ZrO_2 impurity, has been previously structurally refined from room temperature neutron diffraction data collected at Argonne National Laboratory. Conductivity measurements show a cusp at ca. 170°C attributed to the monoclinic–rhombohedral transition and the purpose of this work was to explore the nature of the transition. Data runs were made at 143, 173, 202, 300, and 391°C. No evidence for a crystal system change was found. The highest temperature data sets could not be refined satisfactorily by the Rietveld method using a rhombohedral model, but rather required a monoclinic cell in space group $C2/c$ to achieve convergence. An explanation for the conductivity cusp is given in terms of a disordering of the sodium ions and a change in conduction pathways which lowers the barriers to ion movement.

Introduction

The NASICON family of compounds has attracted wide scientific interest as a prototype example of fast ion transport through a three-dimensional network of channels formed by a rigid oxide network. NASICON was initially formulated as a solid solution of the general formula $Na_{1+x}Zr_2Si_xP_{3-x}O_{12}$ (*1*, *2*). The rigid oxide network provides four cavities per formula within which the conducting cations reside (*2*, *3*). For the end member with $x = 0$, one cavity is filled and three are empty, but the sodium ion conduction is low because of the high barrier blocking movement into the empty cavities. Both end members have rhombohedral crystal structures (*3*, *4*) in space group $R\bar{3}c$. As x increases the additional sodium ions fill empty cavity

* Dedicated to John B. Goodenough.

† Author to whom all correspondence should be addressed.

0022-4596/88 $3.00

sites, but at the same time the passageways between cavities become larger as Si^{4+} replaces P^{5+}. As a result the conductivity increases, reaching a maximum at $x \approx 2$. In the range of highest conductivity $1.6 < x < 2.3$, the structure is monoclinic, space group $C2/c$.

It is now almost certain that crystalline single-phase nonstoichiometric forms of NASICON exist (*5–7*). By nonstoichiometric, we mean compositions which deviate significantly from Hong's formula. Although these phases require that the compositional formulation of NASICON be enlarged to include them (*6*), their structures are such as to not fundamentally alter the basis for fast ion transport described above (*7*). What is now required are definitive statements, based upon structural information, describing the conduction pathways in each of the phases. Hong's original studies (*2*) led him to postulate that the conduction path leads through both sites in the rhombohedral phase [Na(1)–Na(2)–Na(1)] and through all three sodium ion sites in the monoclinic phases. In contrast a single-crystal X-ray study at elevated temperatures of the silicate end member $Na_4Zr_2Si_3O_{12}$ led to the conclusion that the main conduction pathway is from Na(2) to Na(2) sites (*8*). A subsequent single-crystal X-ray study of nonstoichiometric preparation (*9, 10*), with $x = 1.4$, clearly demonstrated that at sufficiently high temperature (222°C) the conduction pathway is Na(1) to Na(2).

A neutron diffraction study (*11, 12*), carried out on powders with different x values, offered an explanation as to both the increase in the c axis with increasing Si content and the conductivity behavior. As silicate tetrahedra replace phosphate tetrahedra, they tilt in such a way as to enlarge the c axis and open the bottlenecks. This process reaches a maximum at about $x = 2$ and thereafter the c axis decreases in length, thereby increasing the barrier to diffusion. A follow-up neutron diffraction study was carried out at 320°C for the two powders with $x = 1.6$ and $x = 2.0$ (*13*). Only slight shifts in atoms occurred, so that no clear picture as to why a phase transformation from monoclinic to rhombohedral should occur at about 180°C emerged from the study. A similar neutron diffraction study carried out on NASICON powders with $x \approx 1$ and 2 yielded similar results (*14*), but with some real differences in sodium site occupancies. For example, in the $x = 2$ sample of Baur *et al.* (*14*), the occupancies (at 300°C) were 40% for the Na(1) sites and 57% for the Na(2) sites as compared to 100 and 66%, respectively, in the Didisheim study (*13*). It should be noted that the composition of Baur's compound was given as $Na_{3.31}Zr_{1.91}Si_{2.01}P_{0.99}O_{11.97}$ and that refinement of occupancy factors for sodium ions yielded no more than two-thirds of the required number (*14*). This composition and sodium ion distribution is in agreement with that proposed previously by Clearfield and co-workers (*15, 16*). As will be shown in this report, we also could only account for about two-thirds occupancy of the sites by the sodium ions. An explanation for these discrepancies has not yet been forthcoming, but a clue as to its origin can be gleaned from a consideration of the monoclinic–rhombohedral phase transition which supposedly occurs at elevated temperature (*17, 18*). This phase change has been correlated with the change in slope of the conductivity–temperature plot (*2*), the curve showing a decreased activation energy above the transition temperature. However, thermal studies (*17, 19–21*) indicate a broad transition occurring over a sizable but variable temperature range of 100 to 200°C rather than a sharp first-order type phase transition. The transition enthalpy is also variable and of low magnitude (*19*). Variability in the thermal effects is attributed to the different thermal histories of the samples examined (*19*). Accord-

ing to Davies *et al.* (*19*) the variations in the Si–P framework can alter the distribution of Na^+ in the cavities and thus change conductivity behavior. Our work has indeed shown (*15, 16*) that ordering of phosphate and silicate groups can occur and that the structure and properties do depend upon the method of preparation of the solid electrolyte (*22, 23*). Therefore, we have undertaken to assess the effect of cation ordering and temperature on structure and subsequent thermal and conductivity behavior of different NASICONs. In this paper we report on a neutron diffraction examination of a near stoichiometric sample ($x \approx 2$) in the temperature range 25–391°C.

Experimental

A commerically available NASICON (Alfa-Inorganics) which initially contained about 20 wt% unreacted ZrO_2 was reheated to 1100°C for 24 hr, followed by a second treatment at 1150°C for 24 hr. In both cases the sample was cooled slowly by turning off the furnace power and allowing the sample to cool at the same rate as the furnace (~10 hr). This reduced the free zirconia to about 4 wt%. Refinement of the time-of-flight room temperature neutron diffraction powder data yielded a composition based upon occupancy refinement of $Na_{3.17}Zr_{1.93}Si_{1.9}P_{1.1}O_{12}$ (*16*). The sample was analyzed by X-ray fluorescence (Micron, Inc., Wilmington, DE). FOUND: Na, 13.8%; Si, 9.9%; P, 6.3%; Zr, 34.8%. CALCULATED FOR $Na_{3.17}Zr_{1.93}Si_{1.9}P_{1.1}O_{12}$ + 3 wt% ZrO_2: Na, 13.4%; Si, 9.8%; P, 6.25%; Zr, 34.5%. These calculated values gave the best overall agreement with the observed analysis and the room temperature neutron diffraction results. This same sample, referred to as AI-NAS-1, was used in the present study.

Time-of-flight neutron powder data were collected on the special environments powder diffractometer (SEPD) (*24*) at the intense pulsed neutron source (IPNS), Argonne National Laboratory. The sample was loaded into a beam-welded vanadium sample can under an inert dry atmosphere. The can, ca. 5.2 cm^3 in volume, was sealed by a lead gasket. Cadmium shielding was used to eliminate scattering from the end caps of the can and the support fixture. Data were collected at 143, 173, 202, 300, and 391°C using a temperature-programmed furnace with an estimated temperature error of ±1°C. The sample was equilibrated at each new temperature for sufficient time (up to 2 hr) to allow any phase change to occur. Data collection at each temperature required ca. 12 hr. The data used in the refinement were collected on the 150° (backscattering) data banks. The room temperature monoclinic structures (*16*) of both the major NASICON phase and the minor ZrO_2 phase (*25*) were used as the starting point for the 143 and 173°C data sets. In data sets taken at 202, 300, and 391°C, a rhombohedral model was used as the starting point for refinement, for the NASICON phase (*26*). In all cases the Na occupancies were statistically distributed over all the available sites. During the course of the work we found that the Si/P populations at elevated temperature were insensitive to the refinement process and so were fixed in the same ratio as was found to result from the room temperature refinement (*16*).

Rietveld refinement was conducted using programs from the IPNS Rietveld analysis program set which has been described in general elsewhere (*27*). The latest programs were used for data analysis, namely TLSMPH2, which allows up to four phases to be simultaneously refined and includes a modified six-term background function. Refinement was conducted on both phases simultaneously using a VAX 11/780 computer. In all cases positional, thermal and scale factors were refined for both phases together with a six-term background and

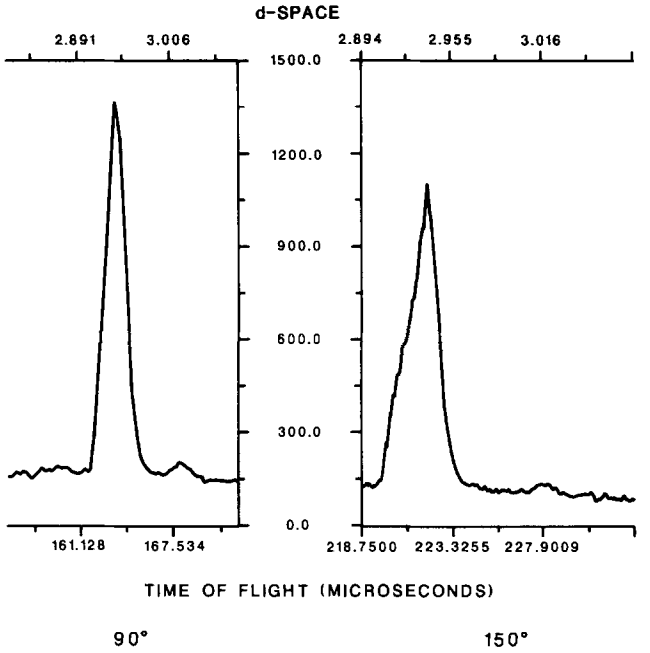

FIG. 1. A portion of the NASICON diffraction pattern obtained at the 90° data banks (left) and 150° data banks (right). The monoclinic distortion is clearly evident at higher resolution (data recorded at 300°C).

six-term peak shape function. The two-term Gaussian peak shape parameters for each phase were also refined. After convergence, populations of the Zr and Na of the NASICON phase were refined followed by anisotropic thermal parameter refinement of the Na atoms.

143 and 173°C Data Sets

Data refinement went smoothly to convergence for both the NASICON and ZrO_2 phases. The Na(3) atom, however, refined into a local minimum for both data sets. The Na atoms were therefore removed; the lattice framework was rerefined and the Na atoms were found by difference Fourier techniques. Final refinement to convergence, population, and anisotropic Na refinement was then easy to accomplish.

220, 300, and 391°C Data Sets

The rhombohedral lattice framework could be refined quickly to convergence, but large residual errors were found in all the refinement plots. Attempts to refine the Na temperature factors or populations resulted in worse residuals and the sodium atoms "blew up." When the sodium atoms were removed, difference Fourier techniques could not relocate them. Critical reexamination of the data showed that in none of these high-temperature data sets had the NASICON changed phase. Figure 1 illustrates this, showing what appears to be a rhombohedral singlet in the 90° detector banks. However, closer inspection revealed that in the backscattering (150°) detector banks this reflection envelope is in fact a quadruplet which can only be indexed in the monoclinic system. A monoclinic framework was thus adopted for all the data sets; the Na atoms were located by difference Fourier techniques on a refined, converged framework model and final convergence as outlined for the lower temperature data sets was readily accomplished.

TABLE I

REFINEMENT PARAMETERS FOR EACH TEMPERATURE

	Temperature (°C)					
	RT[a]	143	173	202	300	391
Space group	*C2/c*	*C2/c*	*C2/c*	*C2/c*	*C2/c*	*C2/c*
a (Å)	15.6451(4)	15.6649(6)	15.6723(9)	15.6764(10)	15.6817(10)	15.6909(9)
b (Å)	9.0491(2)	9.0500(3)	9.0537(6)	9.0520(6)	9.0534(6)	9.0525(5)
c (Å)	9.2151(2)	9.2455(3)	9.2758(4)	9.2844(5)	9.2966(4)	9.3065(4)
β (deg)	123.724(3)	123.905(4)	124.233(6)	124.241(8)	124.207(7)	124.193(7)
Volume (Å^3)	1085.08(3)	1087.86(4)	1088.15(5)	1089.13(6)	1091.53(5)	1093.43(5)
Data range (μsec)			6200–24,000			
Data range (Å)			0.82–3.23			
No. contributing reflections	977/287	991/287	989/288	989/289	989/290	989/289
R_{wp}[b]	0.0334	0.049	0.041	0.045	0.046	0.042
R_P[c]	0.0539	0.106	0.083	0.095	0.103	0.095
R_e[d]	0.0183	0.024	0.023	0.027	0.030	0.025

[a] Ref. (*16*).

[b] $R_{wp} = \left\{\sum_i w_i[Y_i(\text{obs}) - Y_i(\text{calc})]^2 \Big/ \sum_i w_i[Y_i(\text{obs})]^2\right\}^{1/2}$.

[c] $R_P = \sum_i [Y_i(\text{obs}) - Y_i(\text{calc})] \Big/ \sum_i [Y_i(\text{obs}) - bkg_i]$.

[d] $R_e = \sqrt{df} / \sum_i w_i[Y_i(\text{obs})]^2$.

Results

Final refinement parameters for all the data sets are given in Table I. Positional, thermal, and occupancy parameters are given for the five temperatures in Tables II–VI. Important bond lengths and angles are collected in Table VII. A final Rietveld profile plot for one of the five structural refinements is given in Fig. 2 and a schematic drawing of the monoclinic structure is shown in Fig. 3. Refinement results for the 202, 300, and 391°C data sets forced into the rhombohedral model are given in Table VIII.

The most striking feature of our study is the fact that no monoclinic–rhombohedral transformation was found to take place. The data collected at the 90° detectors are well duplicated by use of rhombohedral cell parameters, but not the more highly resolved data from the 150° data bank. It was necessary to invoke a monoclinic model for this purpose. Unit cell parameters resulting from all the Rietveld refinements over the entire temperature range (25–391°C) are listed in Table I. A plot of individual cell lengths against temperature (Fig. 4) all show a change of slope at 205°C but the volume expansion is linear up to 391°C. The volume expansion coefficient is 2.09×10^{-5} °C^{-1}, in good agreement with the value of 2.2×10^{-5} °C^{-1} given earlier (*13*).

No drastic structural changes occur as a result of increased temperature. Na(3) atoms appear to move away from O(3) in symmetry position $\frac{1}{2} + x, \frac{1}{2} - y, \frac{1}{2} + z$ and toward O(3)′ in symmetry position $\overline{xyz}$. The total occupancies of the sodium atom positions are lower than required by the NASICON formula. Furthermore, their temperature factors did not increase with temperature but fluctuated up and down. We attribute this behavior to the disordering of the sodium atoms and the spreading of the sodium atom density over larger volumes at elevated temperatures. Significant amounts of positive density remained

TABLE II

POSITIONAL, POPULATION, AND THERMAL PARAMETERS FOR 143°C REFINEMENT[a]

	x	y	z	B_{iso}/B_{eqv}	Population
Zr	0.0985(4)	0.2554(10)	0.0506(4)	1.24(8)	0.945(7)
P(1)	0.00	0.0405(12)	0.25	0.87(16)	0.49
Si(1)	0.00	0.0405(12)	0.25	0.87(16)	0.51
Si(2)	0.3608(6)	0.1038(12)	0.2634(10)	2.21(16)	0.70
P(2)	0.3608(6)	0.1038(12)	0.2634(10)	2.21(16)	0.30
O(1)	0.1462(6)	0.4312(9)	0.2155(8)	3.11(16)	1.0
O(2)	0.4322(5)	0.4441(9)	0.0816(7)	1.97(11)	1.0
O(3)	0.2578(5)	0.1794(8)	0.2180(7)	2.05(12)	1.0
O(4)	0.3777(5)	0.1343(8)	0.1068(8)	2.56(12)	1.0
O(5)	0.4511(6)	0.1801(8)	0.4326(8)	3.33(15)	1.0
O(6)	0.0775(5)	0.1402(8)	0.2357(8)	2.25(14)	1.0
Na(1)	0.25	0.25	0.50	11.02	0.16(2)
Na(2)	0.50	0.8939(31)	0.25	6.33	0.80(3)
Na(3)	0.8048(24)	0.0826(34)	0.8224(34)	8.30	0.49(4)

	β_{11}[b]	β_{22}	β_{33}	$2\beta_{12}$	$2\beta_{13}$	$2\beta_{23}$
Na(1)	0.011(5)	0.031(8)	0.075(2)	0.011(6)	0.021(9)	−0.046(11)
Na(2)	0.020(2)	0.007(2)	0.047(5)	0.0	0.030(3)	0.0
Na(3)	0.012(2)	0.020(3)	0.055(7)	0.003(3)	0.018(3)	0.002(5)

[a] Figures in parentheses indicate the error in the least significant digit.

[b] The form of the anisotropic temperature factor is $\exp(h^2\beta_{11} + k^2\beta_{22} + l^2\beta_{33} + 2hk\beta_{12} + 2hl\beta_{13} + 2kl\beta_{23})$.

TABLE III

POSITIONAL, POPULATION, AND THERMAL PARAMETERS FOR 173°C REFINEMENT

	x	y	z	B_{iso}/B_{eqv}	Population
Zr	0.1009(5)	0.2542(9)	0.0545(3)	1.69(6)	0.940(6)
P(1)	0.00	0.0377(14)	0.25	0.97(17)	0.49
Si(1)	0.00	0.0377(14)	0.25	0.97(17)	0.51
Si(2)	0.3572(7)	0.1013(13)	0.2500(15)	2.99(15)	0.70
P(2)	0.3572(7)	0.1013(13)	0.2500(15)	2.99(15)	0.30
O(1)	0.1399(6)	0.4350(11)	0.2006(8)	4.67(22)	1.0
O(2)	0.4319(6)	0.4392(11)	0.0844(8)	2.89(15)	1.0
O(3)	0.2543(5)	0.1742(8)	0.2255(8)	1.85(12)	1.0
O(4)	0.3741(5)	0.1380(8)	0.1093(7)	3.33(16)	1.0
O(5)	0.4515(5)	0.1784(9)	0.4332(8)	2.86(14)	1.0
O(6)	0.0802(4)	0.1365(6)	0.2414(7)	1.12(9)	1.0
Na(1)	0.25	0.25	0.50	7.38	0.19(1)
Na(2)	0.50	0.8931(21)	0.25	4.46	0.83(3)
Na(3)	0.8079(17)	0.0478(20)	0.6956(20)	6.96	0.61(4)

	β_{11}	β_{22}	β_{33}	$2\beta_{12}$	$2\beta_{13}$	$2\beta_{23}$
Na(1)	0.023(6)	0.008(7)	0.007(7)	−0.022(7)	0.008(6)	−0.002(4)
Na(2)	0.006(1)	0.013(2)	0.027(3)	0.0	0.008(1)	0.0
Na(3)	0.006(1)	0.017(3)	0.055(6)	0.001(1)	0.015(2)	0.008(2)

TABLE IV

POSITIONAL, POPULATION, AND THERMAL PARAMETERS FOR 202°C REFINEMENT

	x	y	z	B_{iso}/B_{eqv}	Population
Zr	0.1007(6)	0.2536(9)	0.0504(3)	1.67(7)	0.960(6)
P(1)	0.00	0.0361(16)	0.25	0.68(20)	0.49
Si(1)	0.00	0.0361(16)	0.25	0.68(20)	0.51
Si(2)	0.3585(8)	0.1014(15)	0.2538(18)	2.93(18)	0.70
P(2)	0.3585(8)	0.1014(15)	0.2538(18)	2.93(18)	0.30
O(1)	0.1403(7)	0.4321(13)	0.2049(10)	2.99(22)	1.0
O(2)	0.4294(6)	0.4400(11)	0.0847(9)	2.39(16)	1.0
O(3)	0.2538(6)	0.1737(10)	0.2237(10)	1.98(16)	1.0
O(4)	0.3737(6)	0.1339(9)	0.1034(9)	3.09(18)	1.0
O(5)	0.4511(6)	0.1725(10)	0.4295(11)	3.47(19)	1.0
O(6)	0.0806(5)	0.1365(7)	0.2414(10)	1.23(11)	1.0
Na(1)	0.25	0.25	0.50	22.76	0.32(2)
Na(2)	0.50	0.9018(14)	0.25	1.70	0.84(2)
Na(3)	0.8044(16)	0.0451(20)	0.6726(24)	3.88	0.49(3)

	β_{11}	β_{22}	β_{33}	$2\beta_{12}$	$2\beta_{13}$	$2\beta_{23}$
Na(1)	0.033(8)	0.097(19)	0.061(13)	−0.045(10)	0.026(10)	0.025(15)
Na(2)	0.002(7)	0.007(1)	0.008(2)	0.0	0.003(1)	0.0
Na(3)	0.003(1)	0.012(3)	0.024(3)	0.003(1)	0.006(2)	0.006(3)

TABLE V

POSITIONAL, POPULATION, AND THERMAL PARAMETERS FOR 300°C REFINEMENT

	x	y	z	B_{iso}/B_{eqv}	Population
Zr	0.1008(6)	0.2505(10)	0.0539(3)	1.68(7)	0.964(6)
P(1)	0.00	0.0374(14)	0.25	0.47(21)	0.49
Si(1)	0.00	0.0374(14)	0.25	0.47(21)	0.51
Si(2)	0.3588(8)	0.1096(14)	0.2627(14)	2.49(19)	0.70
P(2)	0.3588(8)	0.1096(14)	0.2627(14)	2.49(19)	0.30
O(1)	0.1414(8)	0.4310(15)	0.2067(12)	4.93(31)	1.0
O(2)	0.4280(6)	0.4419(11)	0.0829(10)	2.27(16)	1.0
O(3)	0.2536(6)	0.1738(10)	0.2191(10)	1.67(15)	1.0
O(4)	0.3754(6)	0.1335(10)	0.1036(11)	3.81(20)	1.0
O(5)	0.4520(7)	0.1717(10)	0.4280(13)	2.98(17)	1.0
O(6)	0.0798(5)	0.1373(7)	0.2408(10)	1.53(13)	1.0
Na(1)	0.25	0.25	0.50	25.69	0.38(3)
Na(2)	0.50	0.8995(16)	0.25	2.25	0.78(2)
Na(3)	0.8052(15)	0.0476(20)	0.6740(23)	2.61	0.41(3)

	β_{11}	β_{22}	β_{33}	$2\beta_{12}$	$2\beta_{13}$	$2\beta_{23}$
Na(1)	0.049(13)	0.082(22)	0.055(16)	−0.053(15)	0.026(14)	0.018(18)
Na(2)	0.003(1)	0.009(2)	0.012(2)	0.0	0.005(1)	0.0
Na(3)	0.006(1)	0.006(3)	0.020(3)	0.003(1)	0.003(1)	0.010(3)

TABLE VI

POSITIONAL, POPULATION, AND THERMAL PARAMETERS FOR 391°C REFINEMENT

	x	y	z	B_{iso}/B_{eqv}	Population
Zr	0.1023(6)	0.2531(10)	0.0543(3)	2.02(7)	0.976(6)
P(1)	0.00	0.0391(14)	0.25	0.80(19)	0.49
Si(1)	0.00	0.0391(14)	0.25	0.80(19)	0.51
Si(2)	0.3597(8)	0.1048(14)	0.2596(16)	2.73(18)	0.70
P(2)	0.3597(8)	0.1048(14)	0.2596(16)	2.73(18)	0.30
O(1)	0.1407(7)	0.4324(12)	0.2055(12)	5.13(28)	1.0
O(2)	0.4301(6)	0.4429(10)	0.0827(9)	2.49(15)	1.0
O(3)	0.2537(6)	0.1744(9)	0.2169(10)	2.47(16)	1.0
O(4)	0.3744(6)	0.1286(10)	0.1019(11)	3.81(18)	1.0
O(5)	0.4527(7)	0.1751(9)	0.4274(13)	3.77(19)	1.0
O(6)	0.0802(5)	0.1392(6)	0.2414(10)	1.57(11)	1.0
Na(1)	0.25	0.25	0.50	44.18	0.56(4)
Na(2)	0.50	0.9015(14)	0.25	2.82	0.77(2)
Na(3)	0.8042(18)	0.0407(21)	0.6711(25)	7.89	0.61(4)

	β_{11}	β_{22}	β_{33}	$2\beta_{12}$	$2\beta_{13}$	$2\beta_{23}$
Na(1)	0.110(17)	0.118(26)	0.051(10)	−0.087(16)	0.048(13)	−0.002(15)
Na(2)	0.003(1)	0.009(2)	0.020(3)	0.0	0.007(1)	0.0
Na(3)	0.007(1)	0.026(4)	0.047(4)	0.006(2)	0.013(2)	0.017(4)

TABLE VII

IMPORTANT BOND LENGTHS (Å) AND ANGLES (DEG)

	Temperature (°C)				
	143	173	202	300	391
Zr–O (ave.)[a]	2.077 (37)	2.074 (33)	2.075 (33)	2.072 (29)	2.073 (32)
Zr–O (range)	1.964–2.187	1.990–2.208	1.996–2.206	2.001–2.195	1.997–2.212
P(1)/Si(1)–O (ave.)	1.574 (2)	1.573 (8)	1.576 (18)	1.577 (8)	1.579 (10)
P(1)/Si(1)–O (range)	1.571–1.576	1.565–1.581	1.558–1.594	1.570–1.585	1.570–1.589
P(2)/Si(2)–O (ave.)	1.591 (14)	1.591 (33)	1.593 (16)	1.595 (33)	1.594 (15)
P(2)/Si(2)–O (range)	1.567–1.634	1.566–1.653	1.571–1.639	1.513–1.653	1.554–1.624
Na(1)–Na(2)	3.504	3.491	3.521	3.516	3.525
Na(1)–Na(3)	3.218	3.088	2.982	3.008	2.943
Na(3)–Na(3)	4.219/no	4.718/4.739	4.559/4.713	4.538/4.728	4.616/4.711
Na(2)–Na(3)	4.327	4.460	4.334	4.362	4.325
Na(1)–O(ave.)	2.714 (47)	2.704 (117)	2.695 (98)	2.707 (90)	2.717 (104)
Na(1)–O (range)	2.654–2.752	2.591–2.847	2.588–2.807	2.596–2.793	2.587–2.810
Na(2)–O (ave.)	2.629 (81)	2.650 (98)	2.648 (109)	2.647 (103)	2.643 (109)
Na(2)–O (range)	2.500–2.707	2.507–2.761	2.474–2.735	2.482–2.722	2.481–2.746
Na(3)–O (ave.)	2.574 (182)	2.598 (193)	2.540 (219)	2.591 (191)	2.594 (207)
Na(3)–O (range)	2.352–2.816	2.245–2.778	2.229–2.786	2.252–2.759	2.225–2.799

[a] Average bond value ESDs were determined as $\sigma = [(x_i - \bar{x}_i)^2/(n - 1)]^{1/2}$.

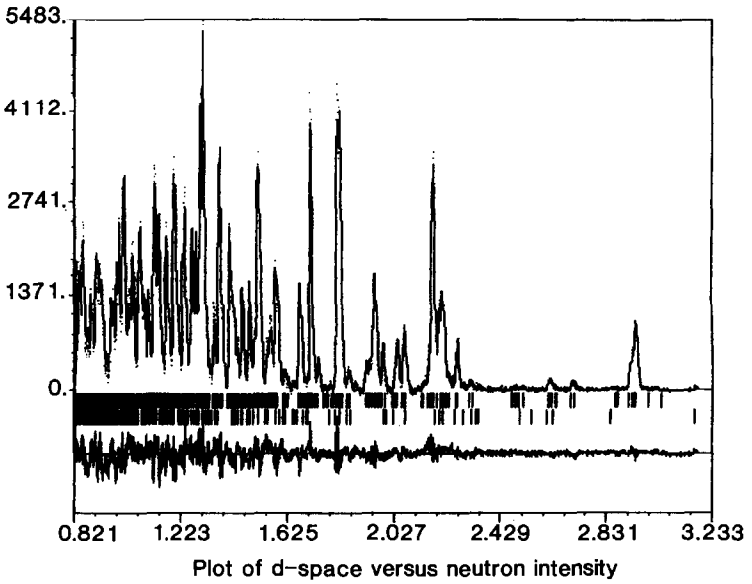

FIG. 2. Final plots of Rietveld refined neutron diffraction data recorded at 143°C on the 150° data banks. Observed data are represented by dots and the calculated pattern is indicated by solid lines. The difference plot is given below. Vertical strikes denote calculated positions of the Bragg reflections with the lower group representing ZrO_2.

in the difference maps to indicate that the thermal ellipsoids did not adequately describe the thermal motion. More elaborate treatment of the thermal parameters was not warranted by the data. A similar underoccupancy of Na was also noted by Baur *et al.* (*14*). Nevertheless, it is clear that the movement of Na(3) is away from Na(1) in such a way as to equalize all the Na(1)–Na(3) interatomic distances. The closest approach of these two ions in the room temperature structure (*16*) is 1.199(7) Å. This value increases to 2.04 (2) Å at 143°C and to about 3 Å at higher temperatures (Table VII).

The foregoing difficulties could possibly indicate a lower symmetry space group. We therefore attempted to refine the 300°C data in space group *Cc*. Not only did R_{wp} increase to 0.049, but two of the sodium atom temperature factors became nonpositive definite. All the bond distances, collected in Table VIII, are regular and show very little change with temperature. Taking as model lengths the value of 1.625 Å for an Si–O bond and for a P–O bond 1.515 Å (*14*), we calculate expected bond lengths of 1.572 and 1.592 Å for the average Si/P–O bond distance in type T1 and T2 sites, respectively. These values agree extremely

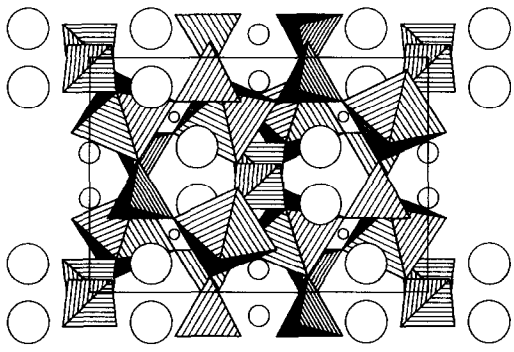

FIG. 3. Schematic projection of the monoclinic NASICON structure in the *ab* plane. Open circles represent sodium ions: Na(1), smallest circles; Na(2), intermediate size circles; Na(3), largest circles.

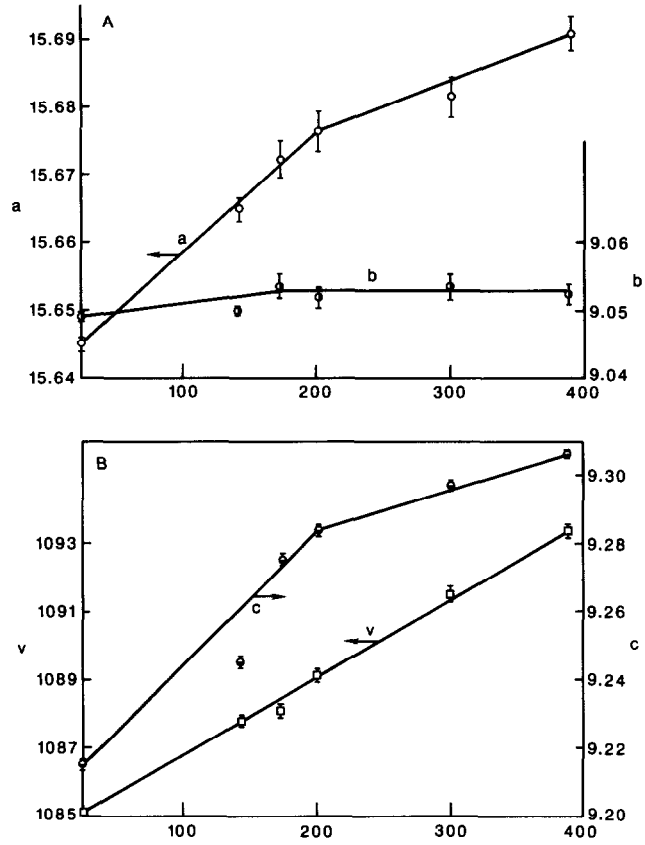

FIG. 4. Plot of cell dimensions and volume of the monoclinic NASICON cells as a function of temperature. (A) Data for a and b axes. (B) Data for c axis and volume. Error bars represent 3 ESDs of the neutron refined data.

well with the observed bond distance (Table VII).

Since no first-order phase change (monoclinic to rhombohedral) was observed there is still a need to explain the change in slope of the conductivity curves and the heat effect which is observed in the same region of temperature. What we observe are small shifts in the tetrahedral groups which enlarge some of the cavity passageways. Examination of the average Na–O bond distances indicates that they generally increase to a maximum at 172°C and then remain relatively constant. (The room temperature values are Na(1)–O 2.696 Å; Na(2)–O 2.615 Å; and Na(3)–O 2.564 Å.) The Na(1)–O interatomic distance actually attains a maximum at 143°C and then decreases to 202°C where once again the distance increases. The sum of the ionic

TABLE VIII

RHOMBOHEDRALLY REFINED MODELS

	Temperature (°C)		
	202	300	391
Space group	$R\bar{3}c$	$R\bar{3}$	$R\bar{3}c$
a (Å)	9.0510(1)	9.0534(1)	9.0557(1)
c (Å)	23.0263(6)	23.06554(6)	23.0935(6)
V (Å^3)	1633.59(4)	1637.25(4)	1640.08(4)
R_{wp}	0.059	0.061	0.057
R_p	0.126	0.134	0.131
R_e	0.027	0.030	0.025

radii Na–O for a six-coordinate sodium is 2.40 Å and for eight-coordination is 2.56 Å (*28*). The average bond distances exceed these values (although for Na(2)–O (ave) this amounts to less than 0.1 Å) and indicate some freedom of movement for sodium ions within the cavities. At room temperature the largest opening or distance between oxygen atoms surrounding the line or centers between sodium atoms is greater than 4 Å, indicating a Na(1)–Na(3)–Na(1) conduction pathway (*16*). However, as temperature increases the pathway between Na(2) and Na(3) also opens from 3.7 to 4.0 Å and an Na(3)–Na(3) passageway increases from 3.37 to 3.8–3.9 Å. Thus, we propose that the change of slope in the conductivity curve results from the creation of new conduction pathways with a concomitant decrease in activation energy. Since these changes occur over a temperature range, they take on the appearance of a second-order phase change, without a change of symmetry.

TABLE IX

COMPARISON OF NEAR STOICHIOMETRIC NASICON UNIT CELL DIMENSIONS

Parameter	Baur *et al.* (*14*)	This work	Didisheim *et al.* (*13*)
Monoclinic unit cell at room temperature			
a	15.6513(17)	15.6451(4)	15.6407(6)
b	9.0550(3)	9.0491(2)	9.0498(3)
c	9.2198(11)	9.2151(2)	9.2102(4)
β	123.742(5)	123.724(3)	123.709(3)
Rhombohedral cells at 300°C			
a	9.0580(4)	9.0534(1)	9.0535(7)[a]
b	23.0705(7)	23.0655(2)	23.0677(2)

[a] T = 320°C.

Discussion

Several high-temperature X-ray and neutron diffraction studies of NASICON phases have now been carried out (*9, 10, 13, 14, 29*). However, in only two of these studies (*13, 14*) was the room temperature phase monoclinic. In both cases the authors reported a monoclinic–rhombohedral transition. The room temperature monoclinic unit cell dimensions for the three separate studies are very close to each other as shown in Table IX. The small deviations among the three preparations may be attributed to small differences in composition. Conversion of our monoclinic values to rhombohedral cell dimensions show a slow but steady convergence of a and b to 300°C where the values are a = 9.0538(6), b = 9.0534(4), c = 23.0625(3) Å. At this temperature $a = b$ within one standard deviation, so that unless the highest resolution is attained, the two crystallographic systems are indistinguishable. However, a and b diverge both above and below this temperature. Our structural results agree very well with those of Baur *et al.* (*14*), even though they refined their data on a rhombohedral model; but they differ in some important respects from those of Didisheim *et al.* (*13*). The latter authors found that the Na(1) site is completely occupied and that there is no deficiency of Zr in their preparation based upon site occupancy of refinement. In contrast we always find a heavy underoccupancy of the Na(1) site and a slight deficiency of Zr. We attributed this underoccupancy to a correlation of the Na^+ occupancy of sites 1 and 3, the sum of the occupancy factors for both sites being approximately one at room temperature (*7, 16*). At elevated temperatures the Na^+ ions spread throughout all the cavity sites.

There is now too much evidence for nonstoichiometry in NASICONS to disregard. We have prepared a highly nonstoichiometric NASICON by a hydrothermal route (*5, 7*) and a sol–gel procedure (*16*). Neither of these preparations contained ZrO_2 or a glassy phase. We even showed that $NaZr_2(PO_4)_3$ was nonstoichiometric (*30*) and this has recently been confirmed by a single-crystal study (*29*). Thus, we have advocated enlarging Hong's formula to encompass these stoichiometries (*6*),

viz., $Na_{1+x+4y}Zr_{2-y-z}Si_xP_{3-x}O_{12-2z}$. Furthermore, we proposed that the differences in stoichiometry depended upon the synthetic method by which the NASICON was prepared (*22*) and in a recent paper deduced evidence to substantiate this claim (*23*). Colomban has presented spectroscopic and X-ray data to show that the degree of ordering of the tetrahedral groups in NASICON depends upon the method of preparation and annealing time (*31*). This degree of ordering affects the conductivity and thermal behavior. We contend that these differences are also reflected in X-ray and neutron structural studies (*16, 22*), but the question remains whether these structural differences are great enough to induce a monoclinic–rhombohedral phase change in some preparations and not in others, or whether this first-order phase transformation in fact does not exist. Therefore we propose to examine the effect of temperature upon NASICON prepared in a variety of ways. Sufficient data will be collected to assess whether framework order and framework-mobile ion interactions indeed can account for the observed thermal and conductivity behavior as suggested by Davies *et al.* (*19*).

Acknowledgments

The Intense Pulsed Neutron Source (IPNS) is operated under the auspices of the U.S. Department of Energy, BES-Materials Sciences, under Contract W-31-109-Eng-38, to whom thanks are extended for the use of their facilities. The portion of this work done at Texas A&M University was supported by a grant from the Texas A&M University Center for Energy and Mineral Resources, for which grateful acknowledgment is made.

Note added in proof. While this manuscript was in press, we became aware of an NMR study on NASICON with $x = 1.9$ (*32*). The sodium resonance is dominated by dynamic second order quadruple interactions. However, the temperature and frequency dependence of the dipolar–quadrupolar linewidths for the $m = \frac{1}{2}$ to $-\frac{1}{2}$ transition fails to uncover evidence for a phase change at elevated temperatures.

References

1. J. B. Goodenough, H. Y.-P. Hong, and J. A. Kafalas, *Mater. Res. Bull.* **11,** 203 (1976).
2. H. Y.-P. Hong, *Mater. Res. Bull.* **11,** 173 (1976).
3. L. Hagman and P. Kierkegaard, *Acta Chem. Scand.* **22,** 1822 (1968).
4. R. G. Sizova, A. A. Voronkov, N. G. Shumyatskaya, V. V. Ilyukin, and N. V. Belov, *Sov. Phys. Dokl.* **17,** 618 (1973).
5. A. Clearfield, P. Jerus, and R. N. Cotman, *Solid State Ionics* **5,** 301 (1981).
6. A. Clearfield, M. A. Subramanian, W. Wang, and P. Jerus, *Solid State Ionics* **9/10,** 895 (1983).
7. P. R. Rudolf, M. A. Subramanian, A. Clearfield, and J. D. Jorgensen, *Mater. Res. Bull.* **20,** 643 (1985); **21,** 1137 (1986).
8. D. Tranqui, J. J. Caponi, J. C. Joubert, and R. D. Shannon, *J. Solid State Chem.* **39,** 219 (1981).
9. H. Kohler and H. Schulz, *Mater. Res. Bull.* **20,** 1416 (1985).
10. H. Kohler, H. Schulz, and O. Melnikov, *Mater. Res. Bull.* **18,** 1143 (1983).
11. B. J. Weunsch, L. J. Schioler, and E. Prince, *in* "Proceedings, Conf. High Temperature Solid Oxide Electrolytes, Brookhaven National Laboratory, Aug. 16–17, 1983," Vol. II, p. 59.
12. L. J. Schioler, Ph.D. dissertation, Mass. Inst. Tech., Cambridge, MA (1983).
13. J. J. Didisheim, E. Prince, and B. J. Wuensch, *Solid State Ionics* **18/19,** 944 (1986).
14. W. H. Baur, J. R. Dygas, D. H. Whitmore, and J. Faber, *Solid State Ionics* **18/19,** 935 (1986).
15. A. Clearfield, M. A. Subramanian, P. Rudolf, and A. Moini, *Solid State Ionics* **18/19,** 13 (1986).
16. P. R. Rudolf, A. Clearfield, and J. D. Jorgensen, *Solid State Ionics* **21,** 213 (1986).
17. U. von Alpen, M. F. Bell, and W. Wichelhaus, *Mater. Res. Bull.* **14,** 1317 (1979).
18. J. P. Boilot, J. P. Salanie, G. Desplances, and D. Le Potier, *Mater. Res. Bull.* **14,** 1469 (1979).
19. P. K. Davies, F. Garzon, T. Feist, and C. M. Katzon, *Solid State Ionics* **18/19,** 1120 (1986).
20. J. P. Boilot, G. Collin, and R. Comes, *Solid State Ionics* **5,** 307 (1981).
21. J. P. Boilot, Ph. Colomban, and G. Collin, *Solid State Ionics* **18/19,** 974 (1986).
22. M. A. Subramanian, P. R. Rudolf, and A. Clearfield, *J. Solid State Chem.* **60,** 172 (1985).
23. A. Moini and A. Clearfield, *Advanced Ceram. Mater.* **2**(2), 173 (1987).

24. J. D. JORGENSEN AND J. FABER, JR., *in* "Proceedings, 6th Mtg. Int. Collab. of Advan. Neutron Sources, Argonne National Laboratory, June 28–July 2, 1982" (J. M. Carpenter, Ed.), pp. 105–114 (ANL publication ANL-82-80).

25. J. D. MCCULLOUGH AND K. N. TRUEBLOOD, *Acta Crystallogr.* **12,** 507 (1959).

26. H. KOHLER AND H. SCHULZ, *Solid State Ionics* **9/10,** 795 (1983).

27. R. B. VON DREELE, J. D. JORGENSEN, AND C. G. WINDSOR, *J. Appl. Crystallogr.* **15,** 581 (1982).

28. C. T. PREWITT AND R. D. SHANNON, *Trans. Amer. Crystallogr. Assoc.* **5,** 57 (1969).

29. H. KOHLER AND H. SCHULZ, *Mater. Res. Bull.* **21,** 23 (1986).

30. A. CLEARFIELD, R. GUERRA, A. OSKARSSON, M. A. SUBRAMANIAN, AND W. WANG, *Mater. Res. Bull.* **18,** 1561 (1983).

31. PH. COLOMBAN, *Solid State Ionics* **21,** 97 (1986).

32. D. T. AMM AND S. L. SEGEL, *Solid State Ionics* **8,** 155 (1983).